Supplemental Figure S1-S7

Physical and hydrodynamic properties of deep sea mining-generated, abyssal sediment plumes in the Clarion Clipperton Fracture Zone (eastern-central Pacific)

Benjamin Gillard[1, 2, *], Kaveh Purkiani [1], Damianos Chatzievangelou [2], Annemiek Vink [3], Morten H. Iversen [1], Laurenz Thomsen [2]

[1] MARUM - Center for Marine Environmental Sciences, University of Bremen, Bremen, Germany; [2] Jacobs University, Bremen, Germany; [3] BGR, Bundesanstalt für Geowissenschaften und Rohstoffe, Hannover, Germany

* b.gillard@jacobs-university.de / bgillard@marum.de

List of Contents:

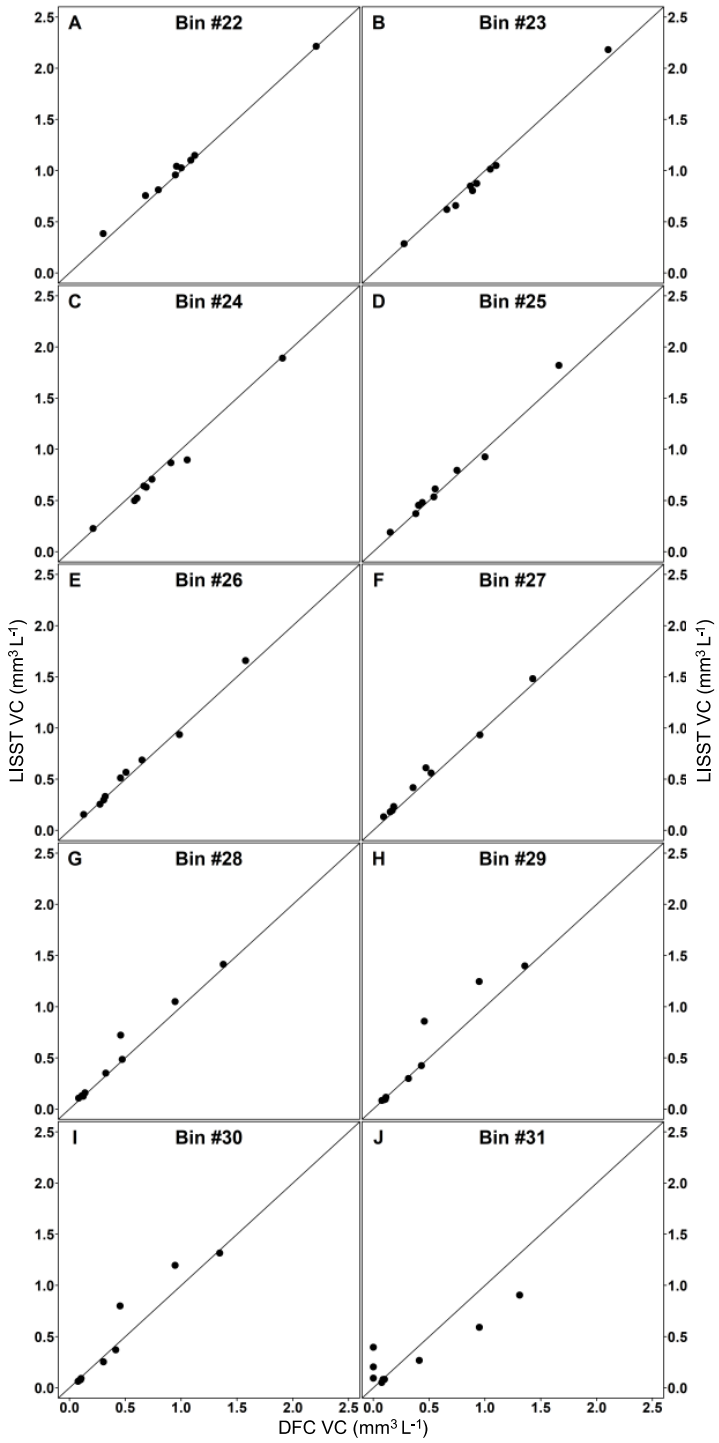

28

29 **Figure S1. Relationships between the volume concentration (VC) from the LISST and**
30 **corrected VC from the camera.**

31 (A-J): Volume concentration for each of the ten overlapping size bins used during the merging
32 procedure (#22–31). Bins size class descriptions are provided in Table S2.

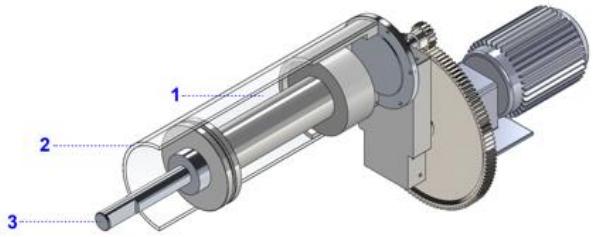

Figure S2. **Schematic drawing of the Couette chamber used for aggregation of sediment under variable shear rate.**
(**1**) Annular space of 2 cm; (**2**) rotating outer Plexiglas cylinder diameter of 12.5 cm; (**3**) Fixed inner cylinder diameter of 8.5 cm. Total working volume of 1.7 L.

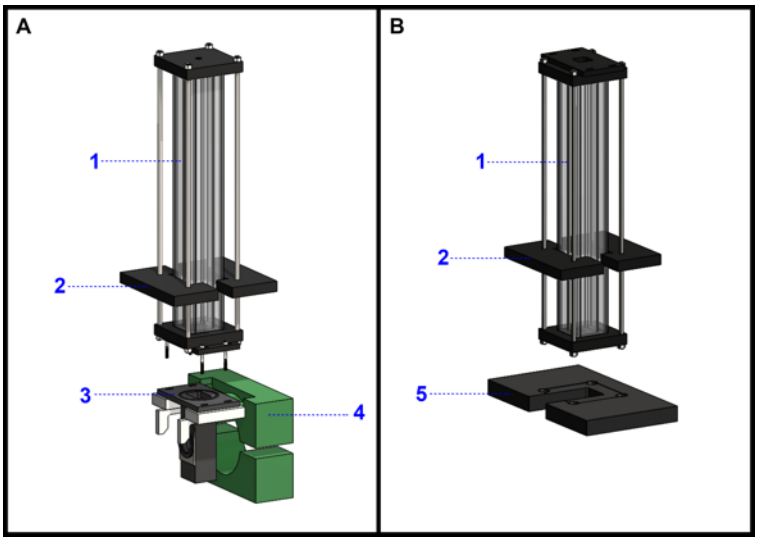

Figure S3. Schematic drawing of the settling column.

The design allows the column to be used either with the LISST-100X (**A**) or separately (**B**). (**1**) 50 cm high settling column; (**2**) light holder; (**3**) measuring section of the LISST-100X; (**4**) LISST-100x fixation clamp; and (**5**) plate holder for separate use.

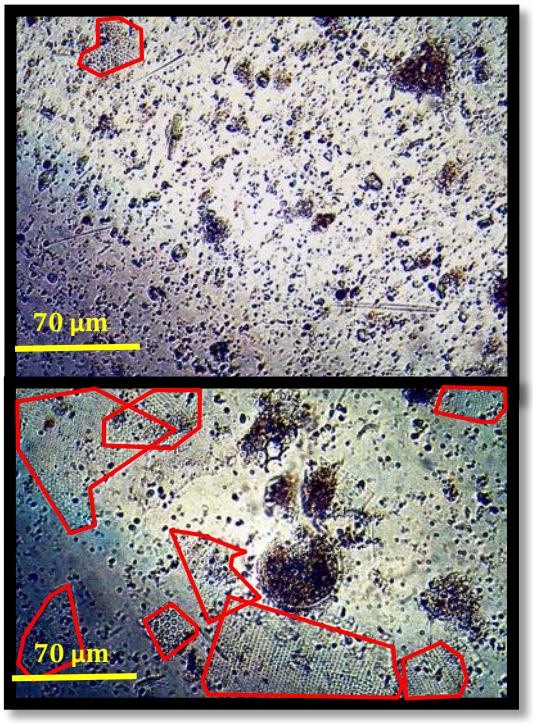

Figure S4. Microscopic pictures of sediment surface layer.
Top picture: sample 95 MUC located in a plain environment. Bottom picture: sample 106 MUC located next to a seamount. Red outlines indicate biogenic deposits including foraminiferal and diatom residues.

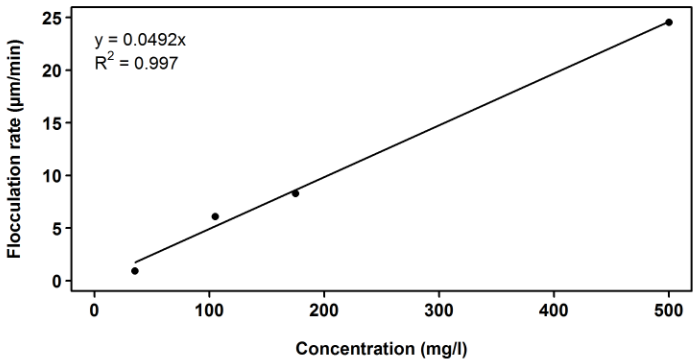

63

64 **Figure S5. Comparison of flocculation rate against sediment plume concentration under**
65 **differential settling (G = 0 s^{-1}).**

66

67

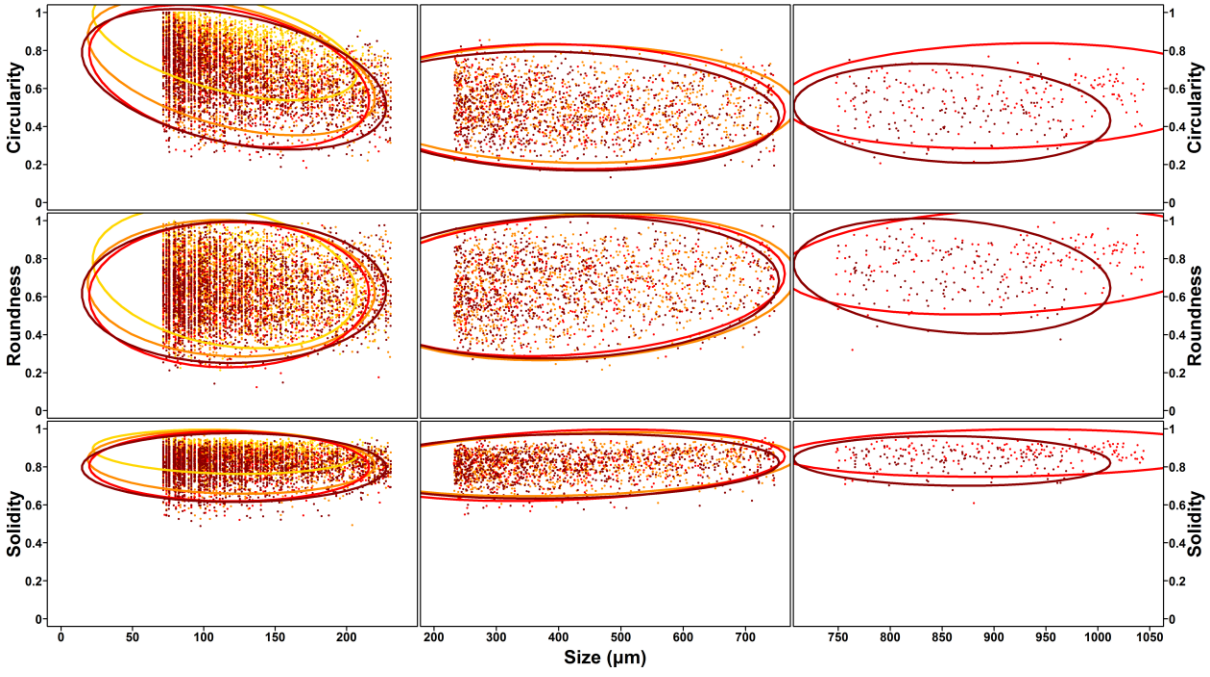

68

69 **Figure S6. Morphological analysis of aggregates produced from variable sediment plume**
70 **concentration under differential settling condition.**
71 Starting sediment plume concentration of: (yellow) 35 mg L^{-1}; (orange) 105 mg L^{-1}; (red) 175 mg
72 L^{-1}; and (brown) 500 mg L^{-1}. Ellipse shape represent 95 % of the data for each sediment
73 concentrations.

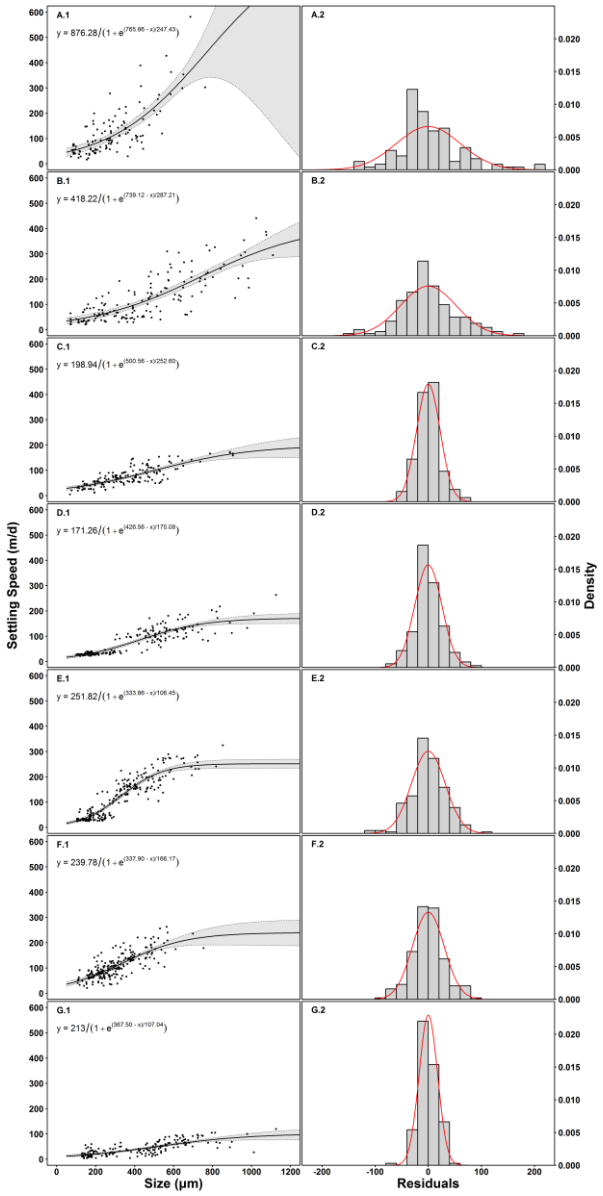

74

75 **Figure S7. Fitted model equation of settling velocities from deep-sea sediment plume**
76 **aggregates.**

77 Settling velocities of aggregates produce under 0 G for a starting sediment plume concentration
78 of: (**A**) 35 mg L^{-1}; (**B**) 105 mg L^{-1}; (**C**) 175 mg L^{-1}; (**D**) 500 mg L^{-1}. Settling velocities of
79 aggregates produce under 2.4 G for a starting sediment plume concentration of: (**E**) 105 mg L^{-1};
80 (**F**) 175 mg L^{-1}; (**G**) 500 mg L^{-1}. Left column: (**.1**) combined raw data and predicted model curve
81 with corresponding 95 % confidence interval. Right column: (**.2**) model residual histogram with
82 plotted normal curve distribution.